

# Controlling of Multi-Level Inverter under Shading Conditions Using Artificial Neural Network

Abed Sami Qawasme, Sameer Khader

**Abstract**—This paper describes the effects of photovoltaic voltage changes on Multi-level inverter (MLI) due to solar irradiation variations, and methods to overcome these changes. The irradiation variation affects the generated voltage, which in turn varies the switching angles required to turn-on the inverter power switches in order to obtain minimum harmonic content in the output voltage profile. Genetic Algorithm (GA) is used to solve harmonics elimination equations of eleven level inverters with equal and non-equal dc sources. After that artificial neural network (ANN) algorithm is proposed to generate appropriate set of switching angles for MLI at any level of input dc sources voltage causing minimization of the total harmonic distortion (THD) to an acceptable limit. MATLAB/Simulink platform is used as a simulation tool and Fast Fourier Transform (FFT) analyses are carried out for output voltage profile to verify the reliability and accuracy of the applied technique for controlling the MLI harmonic distortion. According to the simulation results, the obtained THD for equal dc source is 9.38%, while for variable or unequal dc sources it varies between 10.26% and 12.93% as the input dc voltage varies between 4.47V nd 11.43V respectively. The proposed ANN algorithm provides satisfied simulation results that match with results obtained by alternative algorithms.

**Keywords** Multi level inverter, genetic algorithm, artificial neural network , total harmonic distortion.

## I. INTRODUCTION

PHOTOVOLTAIC power is considered as one of the most important renewable energy sources [1] that to be converted into alternative current form (AC) in order to be connected to the local electrical network at desired voltage and frequency or to energize isolated loads.

Inverters are power converters that are used to convert the input DC voltage into AC voltage with predetermined voltage and frequency. Inverters can be classified into voltage-source, current-source and resonant inverters [2]. Furthermore, in the same class they can be found as single-phase and multi-phases with various control strategies to improve the inverter performances such as sinusoidal pulse width modulation (SPWM), space vector modulation (SVPWM), delta modulation, and recently artificial GA are used to achieve high quality signals.

Recently, MLI are classified as voltage source inverters mainly applied in medium and large power applications in order to reduce the voltage stress on the power switches, and to

A. Abed Sami Qawasme is master student in Renewable Energy & Sustainability Program at Palestine Polytechnic University.

B. Sameer Khader is a Director of Power Electronics & Signal Processing research unit at Palestine Polytechnic University, Hebron, West Bank, Palestine. He is a professor at Department of Electrical Engineering, (e-mail: sameer@ppu.edu).

minimize the THD of the output voltage to be closer to sinusoidal waveform [3]-[10]. In contrary, conventional power inverters are capable to produce two levels of output voltage [11].

It is worth mentioning that when shading conditions occurs the photovoltaic (PV) system generates different voltage levels energizing the MLI, which in turn causes additional THD generated and voltage stress across the devices. This problem can be solved by applying programmable PWM for Cascaded H-Bridge Multilevel Inverter (CHBMLI) using ANN which responds to any change in level voltage by adjusting the switching angles of MLI in order to maintain minimum THD.

## II. MATHEMATICAL MODELING

The proposed mathematical model can be divided into the following stages:

- Decomposing the output signal into Fourier series, where Fourier coefficients and harmonic orders are identified;
- Set of harmonic elimination equations are formulated;
- GA is applied to determine the required switching angles at certain value of THD;
- ANN algorithm is proposed to train the system how to generate the needed switching angles at any level of source voltage changes; and finally, comparison analysis and discussions.

Way out from the periodic integrable function in the interval  $[0, 2\pi]$  combining sum of sine and cosine functions [12] as expressed in (1)

$$f(x) = \frac{a_0}{2} + \sum_{n=1}^N (a_n \cos(n\omega t) + b_n \sin(n\omega t)) \quad (1)$$

where,  $a_0$ ,  $a_n$  and  $b_n$  are the cosine and sine Fourier coefficients;  $n$  is the harmonic order;  $N$  is largest harmonic number; and  $\omega$  is the angular frequency. Now for the output square waveform of eleven level MLI shown in Fig. 1 with equal (balanced) dc sources the Fourier series can be expressed according to (2):

$$V(\omega t) = \sum_{n=1,3,5}^{\infty} \left[ \frac{4V_{dc}}{n\pi} ((\cos n(\theta_1) + (\cos n(\theta_2) + (\cos n(\theta_3) + (\cos n(\theta_4) + (\cos n(\theta_5)) \sin(n\omega t)) \right] \quad (2)$$

While for unequal DC sources, the output voltage can be expressed as given in (3):

$$V(\omega t) = \sum_{n=1,3,5}^{\infty} \left[ \frac{4}{n\pi} ((V_{dc1} \cos n(\theta_1) + (V_{dc2} \cos n(\theta_2) + (V_{dc3} \cos n(\theta_3) + (V_{dc4} \cos n(\theta_4) + (V_{dc5} \cos n(\theta_5)) \sin(\omega t)) \right] \quad (3)$$

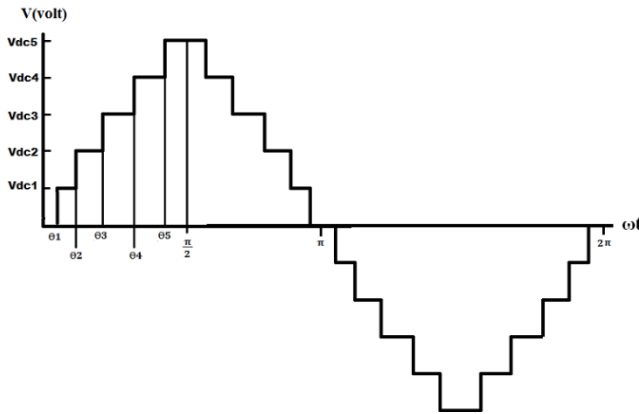


Fig. 1 Output waveform for balanced DC source

The presented five switching angles  $\theta_1$  to  $\theta_5$  are used to formulate the five equations needed to find the fundamental voltage and to minimize the lowest spectrum of harmonics [13] up to 4th order. In unbalanced dc sources modulation index is not targeted since the problem becomes very difficult to be solved. So, the fundamental harmonic will be set to a predetermined value such as 110 V or 120 V as stated in (4):

$$V_1(\text{rms}) = \frac{4}{\sqrt{2}\pi} ((V_{dc1} \cos(\theta_1) + (V_{dc2} \cos(\theta_2) + (V_{dc3} \cos(\theta_3) + (V_{dc4} \cos(\theta_4) + (V_{dc5} \cos(\theta_5))) = 120 \text{ V} \quad (4)$$

In three phase inverters 3rd, 9th and other triple harmonics not existed, while in single phase, these harmonics must be taken into consideration. As previously depicted, the proposed inverter has eleven levels, therefore five equations can be solved to determine the first four harmonics 3rd, 5th, 7th, and 9th in addition to the fundamental harmonic.

While (4) is expressed for the fundamental harmonic, (5) presents the root mean square voltage expression for the high order harmonics.

$$V_3(\text{rms}) = \frac{4}{3\pi\sqrt{2}} ((V_{dc1} \cos(3\theta_1) + (V_{dc2} \cos(3\theta_2) + (V_{dc3} \cos(3\theta_3) + (V_{dc4} \cos(3\theta_4) + (V_{dc5} \cos(3\theta_5))) = 0 \text{ V}$$

$$\dots\dots\dots$$

$$V_9(\text{rms}) = \frac{4}{9\pi\sqrt{2}} ((V_{dc1} \cos(9\theta_1) + (V_{dc2} \cos(9\theta_2) + (V_{dc3} \cos(9\theta_3) + (V_{dc4} \cos(9\theta_4) + (V_{dc5} \cos(9\theta_5))) = 0 \text{ V} \quad (5)$$

### III. GA

GA is a method of optimization and research that can be categorized as an evolutionary algorithm that relies on the imitation of nature's work from a Darwinian perspective [14].

The GA uses a search technique to find controlled or approximate solutions. It is classified as global search heuristics. It is also a specific class of evolutionary algorithms, also known as evolutionary computation, which uses technology inspired by evolutionary biology [15] such as inheritance, mutations, selection and crossover.

In the selective harmonic elimination (SHE) fields, different

analytical solutions were used to keep the fundamental and eliminate the lower-order harmonics such as Newton–Raphson method [16], [17]. But those methods cannot return an answer if there is no exact solution for the equations.

GA operator is used to minimize the voltage THD as much as possible by regulating the obtained set of switching angles in order to obtain best fitness value closed to zero.

The proposed GA is implemented in MATLAB/Simulink with three main modules, fitness file or module, constraints module, and main program module as follows:

- a) Fitness module has the function of minimizing the THD according to (6):

$$\text{THD} = \frac{1}{V_1} \sqrt{\sum_{n=3,5,\dots}^n (V_n)^2} \quad (6)$$

where  $V_1$  is the voltage of fundamental harmonic, and  $V_3, V_5, \dots V_n$  are the voltages of high order harmonics.

- b) Constraints module includes the constraints conditions, where the 3<sup>rd</sup>, 5<sup>th</sup>, 7<sup>th</sup>, and 9<sup>th</sup> harmonic equations are set to zero, taking into account that the switching angles must satisfy the condition expressed in (7):

$$0 < \theta_1 < \theta_2 < \theta_3 < \theta_4 < \theta_5 < \frac{\pi}{2} \quad (7)$$

- c) Main module includes GA operator and parameters such as crossover, mutation, population size and generation.

Many trials of setting parameters and running program had been done so the program does not stop or fall in local minima, and returns best result. It is found that the population size and generation must be changed for each set of input dc voltage such as (800, 70) or (750, 30) respectively, otherwise the algorithm generates incorrect values.

When the program stops, a fitness value of  $6.5 \cdot 10^{-7}$  is obtained having in mind that the exact solution generates zero fitness values. Fig. 2 shows that the approximate and stable solution is achieved after 20 generations.

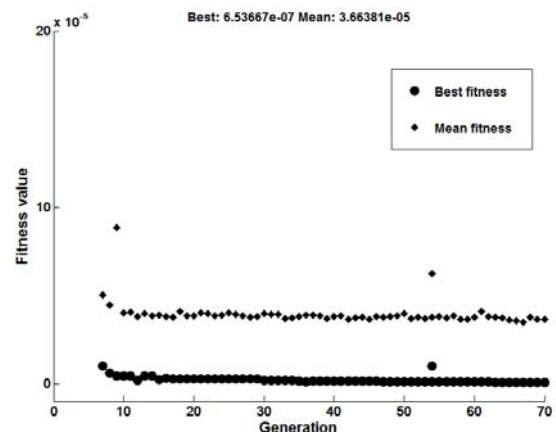


Fig. 2 GA average and best fitness

The output results for sample sets of voltages and their angles are stated in Table I, where the mentioned voltages and angles are used to train the ANN.

TABLE I  
 GA OUTPUT RESULTS

|         | $V_{dc}$<br>(volt) | $\theta$ (degree) |         | $V_{dc}$<br>(volt) | $\theta$ (degree) |
|---------|--------------------|-------------------|---------|--------------------|-------------------|
| unequal | 39                 | 8.560             | unequal | 31                 | 9.093             |
| Vdc     | 38                 | 21.601            | Vdc     | 33                 | 19.384            |
|         | 37                 | 38.131            |         | 35                 | 36.246            |
|         | 36                 | 59.154            |         | 37                 | 58.392            |
|         | 35                 | 88.742            |         | 39                 | 89.000            |
| unequal | 18.35              | 8.772             | equal   | 39                 | 8.738             |
| Vdc     | 22.22              | 14.084            | Vdc     | 39                 | 20.753            |
|         | 27.19              | 18.221            |         | 39                 | 37.421            |
|         | 40.03              | 36.940            |         | 39                 | 58.73             |
|         | 38.56              | 60.202            |         | 39                 | 88.788            |

#### IV. ANN

ANN is a computational technique used to simulate the human brain [18] for dealing with tasks throughout so called massive parallel processing. ANN found widespread applications [19]-[22] in pattern recognition, control systems, classification, etc., where intensive calculations are used to solve nonlinear complicated problems [23].

ANN architecture presents how to connect neurons to each other, relating to the training algorithm. Each neuron has a collector joint that combines the weighted input with the displacement to form the numerical output of the neuron. So instead of using a lookup table to store the large amount of information, ANN is a good alternative to do that.

The problem that can be faced is to know how many hidden layers are needed and how many neurons in each layer are required to train ANN according to the problem input-output relationship. The complexity of relationship between input and output, and their numbers are the main factors that should be determined using trial and error check approach (many attempting).

Taking into account up mentioned constrains, ANN is used to generate a suitable set of switching angles irrespective of the input voltage variations. The final topology was feed forward ANN consisting of two hidden layers as shown in Fig. 3.

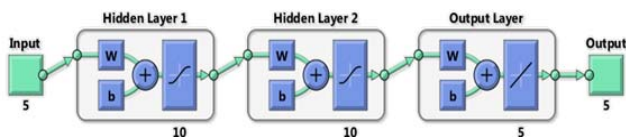


Fig. 3 ANN topology

The network training program is written using MATLAB m-file [23] where a set of parameters is processed to achieve best training. The two hidden layers have 10 neurons with TANSIG activation function for both, while PURELIN activation function is used for the output layer.

The training parameters and algorithms are in continuous change to achieve the best training performance. The training process stopped after 117 iterations where the validation check is achieved as shown on Fig. 4, while Fig. 5 shows the final regression of 99%.

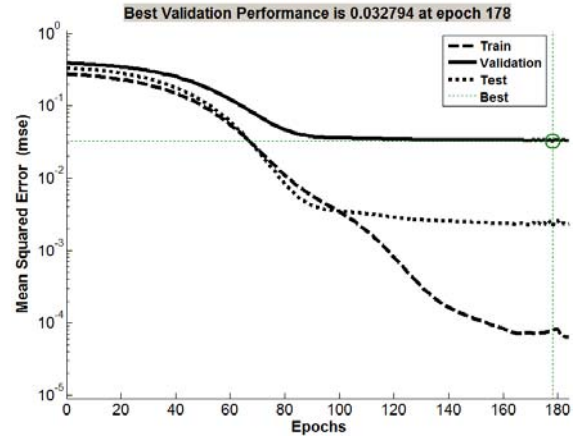


Fig. 4 ANN Training performance

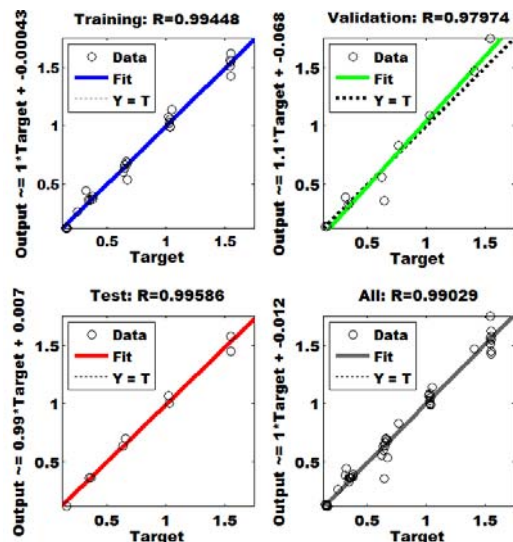


Fig. 5 ANN training regression

#### V. PULSE WIDTH MODULATION

The ANN are trained to produce five switching angles depending on the voltage source levels as shown in Fig. 6 [8], where there are 20 IGBTs formulating eleven levels inverter with  $(2n+1)$  pulses generated by pulse width modulator as shown in Fig. 7 for one cycle.

#### VI. RESULTS AND DISCUSSION

The proposed GA-ANN technique is tested on a single phase 11-level cascade multi-level inverter (CMLI) using MATLAB/Simulink platform.

In the proposed technique, firstly GA is used to solve the nonlinear equations and generate the desired switching angles. Secondly, ANN is trained on the generated angle set produced by the GA, which optimizes the switching angles of 11 level inverter so that 3<sup>rd</sup>, 5<sup>th</sup>, 7<sup>th</sup>, and 9<sup>th</sup> harmonics are minimized.

The output voltages in terms of RMS value and total harmonic distortion depending on the generated switching angles produced by the ANN algorithm are analyzed for different dc voltage levels as follows:

➤ Sources with equal DC voltage are analyzed and stated in Table II, where PV system presenting five dc sources are exposed to the same irradiation levels starting from 1000 W/m<sup>2</sup> to 100 W/m<sup>2</sup> and observing the effect on the output RMS voltage, and THD for 3Ω resistive load. From this

table it is noticed that the obtained THD for equal voltage sources has negligible changes with average value of 9.37% whatever the DC voltage values are changed.

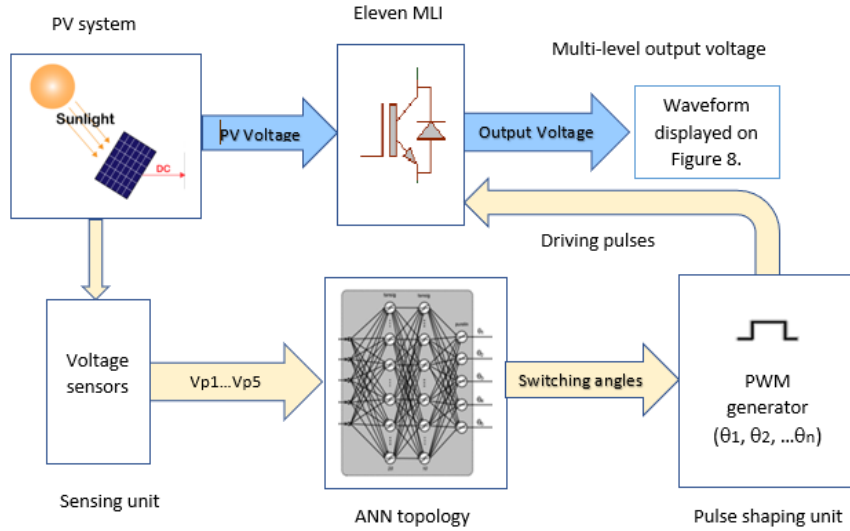


Fig. 6 Pulse generation diagram with ANN topology

TABLE II  
 SET OF FIVE EQUAL DC SOURCES, OUTPUT RMS VOLTAGE, AND THD

| irradiation (W/m <sup>2</sup> ) | PV Source | V <sub>dc</sub> , V | V <sub>RMS</sub> , V | THD % |
|---------------------------------|-----------|---------------------|----------------------|-------|
| 1000                            | v1        | 43.2                |                      |       |
| 1000                            | v2        | 43.2                |                      |       |
| 1000                            | v3        | 43.2                | 124.4                | 9.42% |
| 1000                            | v4        | 43.2                |                      |       |
| 1000                            | v5        | 43.2                |                      |       |
| 800                             | v1        | 42.58               |                      |       |
| 800                             | v2        | 42.58               |                      |       |
| 800                             | v3        | 42.58               | 125.1                | 9.36% |
| 800                             | v4        | 42.58               |                      |       |
| 800                             | v5        | 42.58               |                      |       |
| 500                             | v1        | 41.28               |                      |       |
| 500                             | v2        | 41.28               |                      |       |
| 500                             | v3        | 41.28               | 120.8                | 9.36% |
| 500                             | v4        | 41.28               |                      |       |
| 500                             | v5        | 41.28               |                      |       |
| 100                             | v1        | 36.81               |                      |       |
| 100                             | v2        | 36.81               |                      |       |
| 100                             | v3        | 36.81               | 106.2                | 9.39% |
| 100                             | v4        | 36.81               |                      |       |
| 100                             | v5        | 36.81               |                      |       |

The obtained simulation results for the output voltage and the obtained FFT analysis are illustrated on Figs. 8 and 9 respectively. It is shown that the high order voltage harmonics 3<sup>rd</sup>, 5<sup>th</sup>, 7<sup>th</sup>, and 9<sup>th</sup> are minimized with values less than 1.4% of the fundamental voltage which presents a good indicator for enhancing the inverter performances.

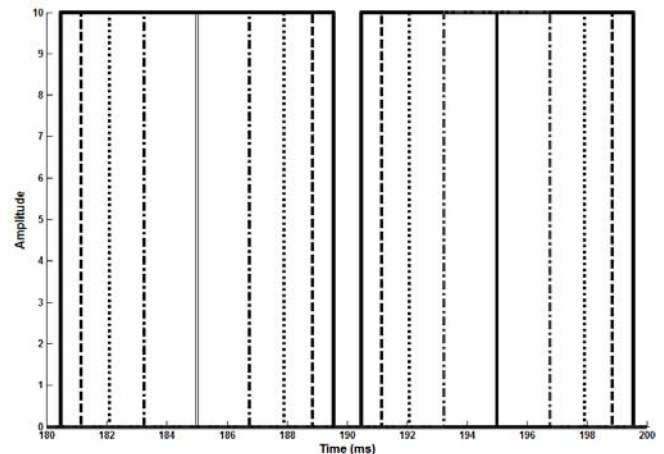


Fig. 7 Projected pulses for one cycle

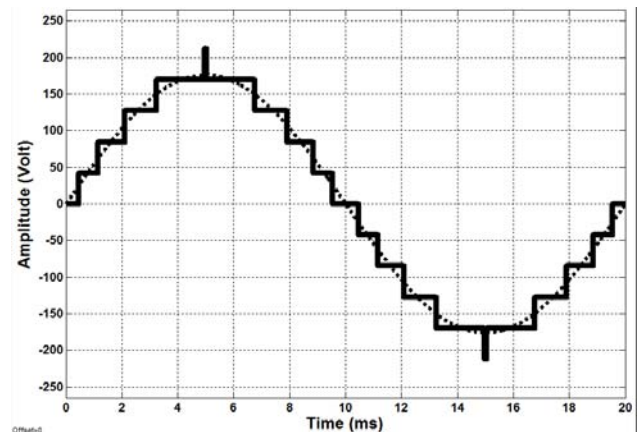


Fig. 8 The output voltage of the CMLI at equal dc sources



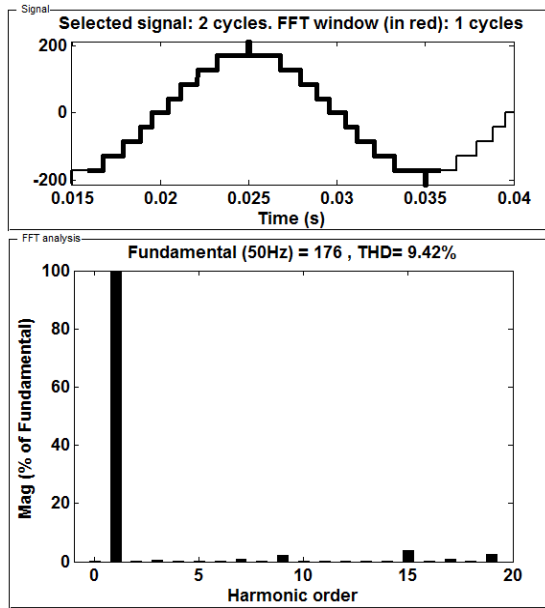


Fig. 9 FFT spectrum of CMLI output voltage at equal dc sources

Sources with unequal DC voltage are analyzed and stated in Table III for the same irradiation levels, the same load and at different shading scenarios, which in turn lead to different values of generated dc voltage. The obtained output RMS voltage of the inverter at unequal dc sources and related FFT are shown on Figs. 10 and 11 for dc voltage variation ranging between 4.47 to 11.43V at 1000 W/m<sup>2</sup> and 100 W/m<sup>2</sup> irradiances respectively.

| TABLE III<br>SET OF FIVE UNEQUAL DC SOURCES, VOLTAGE AND THD |                     |                      |        |
|--|---------------------|----------------------|--------|
| PV Sources   | V <sub>dc</sub> , V | V <sub>RMS</sub> , V | THD %  |
| v1   | 36.81               |                      |        |
| v2   | 36.81               |                      |        |
| v3   | 36.81               | 109.8                | 9.79%  |
| v4   | 41.28               |                      |        |
| v5   | 41.28               |                      |        |
| v1   | 36.81               |                      |        |
| v2   | 36.81               |                      |        |
| v3   | 43.2                | 123.3                | 9.90%  |
| v4   | 43.2                |                      |        |
| v5   | 43.2                |                      |        |
| v1   | 36.81               |                      |        |
| v2   | 36.81               |                      |        |
| v3   | 41.28               | 120.2                | 10.26% |
| v4   | 42.58               |                      |        |
| v5   | 43.2                |                      |        |
| v1   | 24.54               |                      |        |
| v2   | 24.54               |                      |        |
| v3   | 27.52               | 104.4                | 12.88% |
| v4   | 35.46               |                      |        |
| v5   | 35.97               |                      |        |

The FFT analyses of output voltage of both cases are shown in Figs. 12 and 13 respectively.

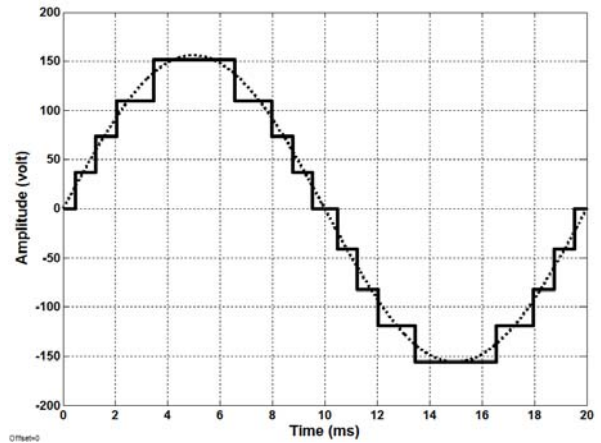


Fig. 10 The output voltage of the CMLI at unequal DC sources (dc variation = 4.47 volts)

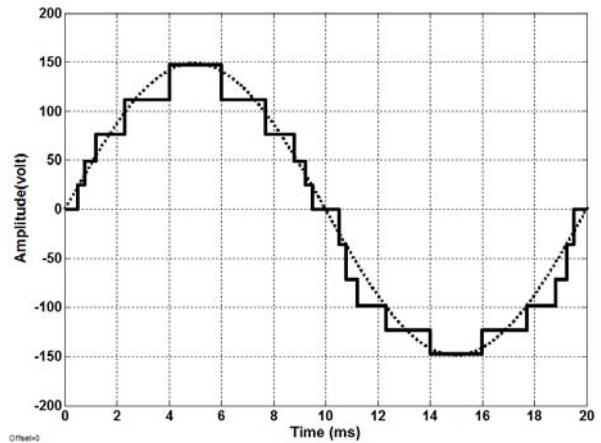


Fig. 11 The output voltage of the CMLI at unequal dc sources (DC variation = 11.43 volts)

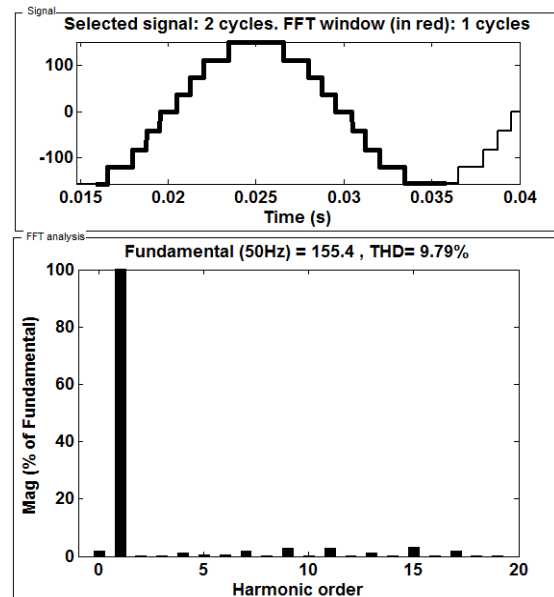


Fig. 12 FFT spectrum of CMLI output voltage at unequal DC sources (dc variation = 4.47 volts)

## VII. CONCLUSION

By applying GA nonlinear equations for selective harmonics elimination were resolved, where GA algorithm has to run many times to get the best solution which in turn needs huge computational time. Despite that the main parameters such as population and generation size, operator and fitness function are optimized, but they have to be set again when the input dc voltages are changed with respect to the applied ANN. It is shown that the output fundamental voltage is kept at fixed value while the high order targeted harmonics are minimized or even eliminated throughout generating different switching angles.

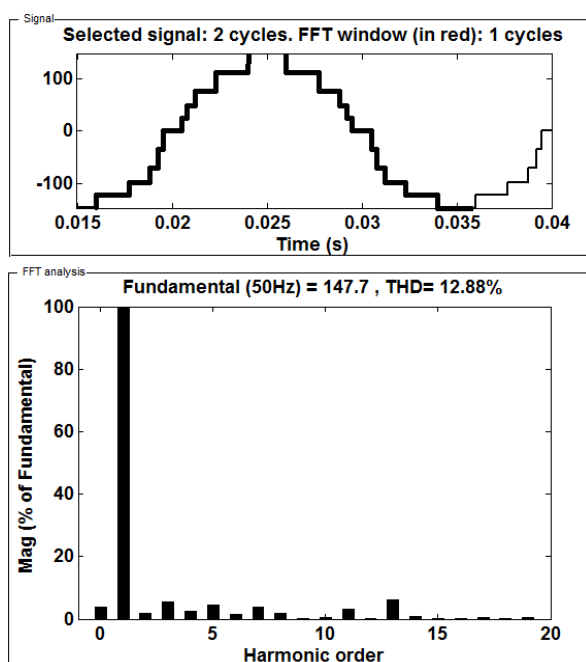


Fig. 13 FFT analysis of CMLI output voltage at unequal dc sources (dc variation = 11.43 volts)

The obtained minimum THD for equal source voltage is 9.36% that matches with similar value obtained by using another GA conducted by other researchers[10]-[13], while for unequal dc sources due to shading conditions, the value of THD becomes 9.90%. Both values are detected at the same irradiation, 800 W/m<sup>2</sup>

Finally, both GA and ANN techniques can be used to minimize the THD for equal and unequal dc sources and can be applied for different kinds of level inverters.

## REFERENCES

- [1] Gilbert M. Masters, *Renewable and Efficient Energy Systems*, 1st edition, 2003, ch.9.
- [2] S. Koura, M. Malinowski, K. Gopakumar, J. Pou, L. G. Franquelo, B. Wu, J. Rodriguez, M. Perez, J. I. Leon, "Recent Advances and Industrial Applications of Multilevel Converters," *IEEE Transactions on Industrial Electronics*, vol. 57, no. 8, pp. 2553-2580, Aug. 2010.
- [3] R. Rangarajan, F. E. Villaseca, "A switching scheme for multilevel converters with non-equal DC sources", 39th North American Power Symposium, pp. 308-313, Sept.2007.
- [4] B. Ozpineci, L. M. Tolbert, J. N. Chiasson, "Harmonic optimization of multilevel converters using genetic algorithms," *IEEE Power Electronics*

- Letters, vol. 3, no. 3, pp. 92-95, Sept. 2005.
- [5] J. N. Chiasson, L. M. Tolbert, K. J. McKenzie, Z. Du, "A unified approach to solving the harmonic elimination equations in multilevel converters," *IEEE Transactions on Power Electronics*, vol. 19, no. 2, pp. 478-490, March. 2004.
- [6] J. N. Chiasson, L. M. Tolbert, K. J. McKenzie, Z. Du, "Elimination of harmonics in a multilevel converter using the theory of symmetric polynomials and resultants," *IEEE Transactions on Control Systems Technology*, vol. 13, no. 2, pp. 216-223, March 2005.
- [7] Z. Du, L. M. Tolbert, J. N. Chiasson, H. Li, "Low switching frequency active harmonic elimination in multilevel converters with unequal DC voltages," *Annual Meeting of the IEEE Industry Applications Society*, pp. 92-98.
- [8] Z. Du, L. M. Tolbert, J. N. Chiasson, "Active harmonic elimination for multilevel converters," *IEEE Transactions on Power Electronics*, vol. 21, no. 2, pp. 459-469, March 2006.
- [9] D. Ahmadi, Jin Wang, "Selective harmonic elimination for multilevel inverters with unbalanced DC inputs," *IEEE Vehicle Power and Propulsion Conference*, pp.773-778, Sept. 2009.
- [10] M. S. A. Dahidah, V. G. Agelidis, "Selective harmonic elimination multilevel converter control with variant DC sources," *IEEE Conference on Industrial Electronics and Applications*, pp. 3351-3356, May 2009.
- [11] J. Rodriguez, J. Lai, F. Z. Peng, "Multilevel inverters: a survey of topologies, control and applications," *IEEE Transactions on Industrial Electronics*, vol. 49, no. 4, pp.724-738, Aug. 2002.
- [12] M. S. A. Dahidah, V. G. Adelids, "Selective harmonic elimination PWM control for cascaded multilevel voltage source converters: A generalized formula," *IEEE Transactions on Power Electronics*, vol. 23, no. 4, pp. 1620-1630, July 2008.
- [13] F. J. T. Filho, L. M. Tolbert, Y. Cao, B. Ozpineci, "Real time selective harmonic minimization for multilevel inverters connected to solar panels using artificial neural network angle generation", *IEEE Energy Conversion Congress and Exposition*, pp. 594-598, Sept. 2010.
- [14] M. Srinivas, L. M. Patnaik, "Genetic algorithms: a survey," *IEEE Computer Society Press.*, vol. 27, no. 6, pp. 17-26, Jun 1994.
- [15] D. E. Goldberg, *Genetic Algorithms in Search, Optimization, and Machine Learning*, MA: Addison-Wesley, 1989.
- [16] K.F. Man, K.S. Tang, S. Kwang, "Genetic algorithms: concepts and applications [in engineering design]," *IEEE Transactions on Industrial Electronics*, vol.43, no.5, pp.519-534, Oct 1996.
- [17] C. R. Houck, J. A. Joins and M. G. Kay, "A genetic algorithm for function optimization: A MATLAB implementation," *Technical Report NCSU-IE-TR-95-09*, North Carolina State University, Raleigh, NC (1995).
- [18] J. J. Hopfield, "Artificial neural networks," *IEEE Circuits and Devices Magazine*, vol. 4, no. 5, pp. 3-10, Sep.1988.129
- [19] R. Aggarwal, Y. Song, "Artificial neural networks in power systems II: types of artificial neural networks," *Power Engineering Journal*, vol. 12, no. 1, pp. 41-47, Feb. 1998.
- [20] R. Aggarwal, Y. Song, "Artificial neural networks in power systems I: general introduction to neural computing," *Power Engineering Journal*, vo. 11, no. 3, pp. 129-134, Jun. 1997.
- [21] M. J. Willis, C. Di Massimo, G. A. Montague, M. T. Them, A. J. Morris, "Artificial neural networks in process engineering," *IEE Proceedings in Control Theory and Applications*, vol. 138, no. 3, pp. 256-266, May 1991.
- [22] A.K. Jain, Jincheng Mao, K. M. Mohiuddin, "Artificial neural networks: a tutorial," *Computer*, vol. 29, no. 3, pp. 31-44, Mar 1996.
- [23] *MATLAB /Simulink User's Guide* , 2016, [www.mathwork.com](http://www.mathwork.com)